

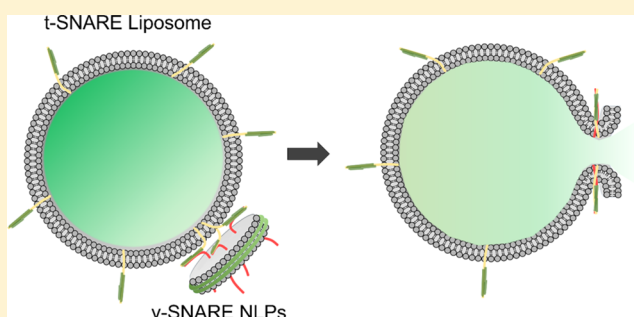
# Using ApoE Nanolipoprotein Particles To Analyze SNARE-Induced Fusion Pores

Oscar D. Bello, Sarah M. Auclair, James E. Rothman,\* and Shyam S. Krishnakumar\*

Department of Cell Biology, Yale University School of Medicine, New Haven, Connecticut 06510, United States

## S Supporting Information

**ABSTRACT:** Here we introduce ApoE-based nanolipoprotein particle (NLP)—a soluble, discoidal bilayer mimetic of ~23 nm in diameter, as fusion partners to study the dynamics of fusion pores induced by SNARE proteins. Using *in vitro* lipid mixing and content release assays, we report that NLPs reconstituted with synaptic v-SNARE VAMP2 (vNLP) fuse with liposomes containing the cognate t-SNARE (Syntaxin1/SNAP25) partner, with the resulting fusion pore opening directly to the external buffer. Efflux of encapsulated fluorescent dextrans of different sizes show that unlike the smaller nanodiscs, these larger NLPs accommodate the expansion of the fusion pore to at least ~9 nm, and dithionite quenching of fluorescent lipid introduced in vNLP confirms that the NLP fusion pores are short-lived and eventually reseal. The NLPs also have capacity to accommodate larger number of proteins and using vNLPs with defined number of VAMP2 protein, including physiologically relevant copy numbers, we find that 3–4 copies of VAMP2 (minimum 2 per face) are required to keep a nascent fusion pore open, and the SNARE proteins act cooperatively to dilate the nascent fusion pore.



## 1. INTRODUCTION

Membrane fusion, in which two distinct lipid membranes are merged into one, is a ubiquitous event critical to a variety of biological processes, including regulated release of neurotransmitters and hormones, intracellular transport of protein and other cargoes, and viral infection.<sup>1–5</sup> All membrane fusion reaction results in a fusion pore—a transient, narrow channel (1–2 nm) that connects the two fusing compartments.<sup>6–8</sup> This dynamic fusion pore may irreversibly widen or close.<sup>6,8</sup> Small cargoes like neurotransmitters might be released through the flickering nascent pore,<sup>9,10</sup> but larger cargoes like hormones and viral genomes require the dilation of the initial fusion pore.<sup>6,11,12</sup> Thus, the fusion pore is the site for regulation by number of biological factors.<sup>13,14</sup> Fusion pore formation is associated with conformational changes in SNARE (soluble N-ethylmaleimide-sensitive factor attachment protein receptor) proteins, which catalyze most of the intercellular fusion events.<sup>15,16</sup> SNARE protein emanating from the transport vesicles (v-SNAREs) assemble with its cognate t-SNAREs on the target membrane bringing the opposing membranes in close proximity and provides the energy to fuse the lipid bilayers and open a fusion pore.<sup>15–18</sup>

Membrane fusion has been typically studied using an *in vitro* assay that monitors the lipid mixing between two liposomes containing reconstituted cognate SNARE proteins.<sup>16,19</sup> This assay has greatly contributed to our understanding of membrane fusion, but it is not well-suited to study fusion pores since the fusion pore is formed between two inaccessible compartments. Modified versions of the liposome fusion assays

using self-quenched volumetric dyes preloaded into the liposomes have been commonly used to monitor fusion pore dynamics.<sup>20–22</sup> However, these assays are not sensitive as they have a very low signal-to-noise ratio. In general, fusion pore dynamics are investigated using sophisticated methods, like patch-clamp electrophysiology/amperometry and high-resolution optical methods.<sup>12,22–25</sup> Though these methods are very sensitive, they require a highly specialized experimental setup and are not easily adaptable to reconstituted systems, which are needed to achieve a mechanistic understanding of fusion pore formation and expansion.

We recently described an assay inspired by the *in vitro* liposome fusion assay, in which one of the liposome is replaced by flat, nanomembranes called nanodiscs (ND) assembled with membrane scaffold protein derived from apolipoprotein A-1.<sup>26,27</sup> In this reconstituted system, the fusion pore opens directly to the exterior medium, making it much easier to probe the properties of the fusion pore. This also allows for a more sensitive and accurate quantitation of the released content.<sup>26,27</sup> Further, the NDs are monodisperse in size and the number of copies of SNAREs (or other fusogens) on the NDs can be rigorously controlled, making it a very reliable and highly reproducible system. The NDs allow the nascent fusion pore to form, and its small size (~16 nm diameter) stabilizes this nascent pore by restricting its expansion.<sup>27</sup> Thus, ND—

**Received:** January 21, 2016

**Revised:** February 24, 2016

**Published:** March 13, 2016

liposome system is well suited to study the formation of the nascent fusion pore, but not the fate of the nucleated pore, in particular the dilation of the nucleated pore and the related parameters.

To address this, we sought to develop new flat, suspended membranes that retain all the advantages of the ND–liposome setup but allow the expansion of the fusion pore. We focused on apolipoproteins other than ApoA1,<sup>28</sup> as it has been demonstrated that a wide range of these apolipoproteins (ApoE, ApoC, ApoB, and apolipoprotein) self-assemble with lipids to form discoidal bilayer patches with the apolipoprotein acting as a scaffold.<sup>29–31</sup> In particular, ApoE has been shown to form polydisperse nanolipoprotein particles (NLP) with discrete sizes ranging from ~15 to 30 nm.<sup>32–34</sup> Modeling and computational analysis have shown that the ApoE is inherently flexible and can adopt three different folded conformations, and the discrete sized particles are related to the structure and number of ApoE surrounding the NLP complex.<sup>33</sup>

Here, we describe methods to template and purify homogeneous NLP complexes of ~23 nm in diameter by controlling the ApoE/lipid ratio. We demonstrate that NLPs carrying VAMP2 (vNLP) are ideally suited to study the fusion pore properties since the fusion pore is externally accessible and the large size of the NLP allows the dilation of the fusion pore, with efficient efflux of cargo up to ~9 nm. We find that an average of 3–4 copies of SNAREs is required open an nascent fusion pore and increasing the number of copies of VAMP2 in the NLP enhance the release of the large cargo, suggesting that several SNAREs might act in concert to expand the fusion pore.

## 2. EXPERIMENTAL SECTION

**2.1. Plasmid Constructs and Protein Purification.** The constructs used in this study are full-length VAMP2 (His<sup>6</sup>-SUMO-VAMP2, residues 1–116);<sup>35</sup> full-length t-SNARE complex (mouse His<sup>6</sup>-SNAP25, residues 1–206 and rat Syntaxin-1, residues 1–288),<sup>16</sup> MSP1E3D1 expression vector (pMSP1E3D1),<sup>27,35</sup> and N-terminal 22 kDa fragment of Apolipoprotein E4 (residues 1–199, with E422K mutation kindly provided by Dr. Nicholas Fischer, Lawrence Livermore National Laboratory, Livermore, CA). VAMP2, t-SNAREs, and MSP proteins were expressed and purified as described previously.<sup>16,35</sup> ApoE422K was expressed and purified as previously described<sup>36</sup> with slight modification. Briefly, ApoE422K (pET32a-Trx-His<sup>6</sup>-ApoE422K) was transformed into *E. coli* strain BL21(DE3), and cells were grown at 37 °C to an OD<sub>600</sub> of 0.8 when protein expression was induced with 1 mM isopropyl  $\beta$ -D-thiogalactoside (IPTG) for 4 h. The cells were lysed by cell disruptor (Avestin, Ottawa, Canada) with three passages at ~15 000 psi in 25 mM HEPES, pH 7.4, 400 mM KCl, 1 mM DTT buffer containing 4% Triton X-100. Lysates were clarified by centrifugation (40K for 45 min) and bound to Ni-NTA agarose (Qiagen, Valencia, CA) for 4 h to overnight at 4 °C. Beads were subsequently washed with 25 mM HEPES, pH 7.4, 400 mM KCl, 1 mM DTT buffer containing 1% Triton X-100, followed by 25 mM HEPES, pH 7.4, 400 mM KCl, 1 mM DTT buffer containing 50 mM imidazole and 1% octylglucoside (OG). The protein was cleaved of the beads using 100 U of human thrombin (Sigma-Aldrich, St. Louis, MO) at 4 °C overnight and eluted in 25 mM HEPES, pH 7.4, 400 mM KCl, 1 mM DTT buffer containing 1% OG. The protein concentration was determined using the Bradford assay (Bio-Rad, Hercules, CA) with bovine serum albumin as the standard. Note: long-term storage of the protein in –80 °C with 10% glycerol affected the efficacy of the protein and so was typically stored at 4 °C and was found to be active for up to 4 weeks.

**2.2. Assembly of ApoE Nanolipoprotein Particle (NLP).** To assemble ApoE nanolipoprotein particles, typically 1 mM lipid mixture of palmitoyl-2-oleoylphosphatidylcholine (POPC):1,2-dioleoylphosphatidylserine (DOPS) at 85:15 mol % (for standard preparation)

was dried under nitrogen flow and followed by vacuum for 1 h. The lipid film was resuspended to 300  $\mu$ L in 25 mM HEPES, pH 7.4, 140 mM KCl, 1% OG. The mixture was vortexed at room temperature (RT) for 1 h followed by the addition of ApoE and vortexed another hour at RT, followed by 2 h at 4 °C. The excess detergent was removed with SM-2 biobeads (Bio Rad, Hercules, CA) incubated overnight at 4 °C with constant mixing. The assembled NLPs were separated from free proteins and lipids by size exclusion chromatography (SEC). The elution peak were then concentrated using Amicon Ultra 50 kDa cutoff centrifugal filter (EMD Millipore, Billerica, MA) units to ~150  $\mu$ L. The final concentration of NLPs (determined by 1% NBD-PE introduced for quantitation) was ~1.5 mM. To obtain NLPs of desirable size and homogeneity, we tested ApoE/lipid ratios of 1:45; 1:120, 1:180, and 1:290. The 1:45, 1:120, and 1:180 NLPs were purified on a Superose 6 SEC column (GE Healthcare, Marlborough, MA) and 1:290 NLP on Sephacryl S-500 column (GE Healthcare, Marlborough, MA). To understand the effect of the lipid composition on the size of the NLPs, we generated NLPs using ApoE/lipid ratio of 1:180 with POPC alone, 1,2-dimyristoyl-*sn*-glycero-3-phosphocholine (DMPC) alone, and a physiological lipid mixture of 35% POPC, 15% DOPS, 20% 1-palmitoyl-2-oleoyl-*sn*-glycero-3-phosphoethanolamine (POPE), 25% cholesterol, 3% 1- $\alpha$ -phosphatidylinositol (PI), and 2% 1- $\alpha$ -phosphatidylinositol-4,5-bisphosphate (PIP2). All lipids were purchased from Avanti Polar Lipids (Alabaster, AL).

**2.3. Characterization of ApoE Nanolipoprotein Particle.** The size of the NLPs were determined using electron microscopy (EM). To do this, 8  $\mu$ L of solution containing NLPs (diluted to ~50  $\mu$ M of lipids) and 1% of BSA (w/v) was adsorbed on carbon-coated 400 mesh copper electron microscopy grids for 5 min. The samples were negatively stained first using a fast rinse (5 s) with 3 drops of 1% of uranyl acetate (w/v), followed by a 1 min incubation with 10  $\mu$ L of 1% of uranyl acetate (w/v) and excess liquid removed using filter paper. The grids were subsequently examined in an FEI Tecnai-12 electron microscope operated at 120 kV. Micrographs of the specimen were taken on a Gatan Ultrascan4000 CCD camera at a magnification of 42 000 $\times$ . The size of the NLPs were calculated from its area by measuring ~200 individual particles using ImageJ software and were estimated to be  $16 \pm 2$ ,  $19 \pm 2$ ,  $23 \pm 2$ , and  $33 \pm 5$  nm for 1:45, 1:120, 1:180, and 1:290 NLP, respectively. The size of the 1:180 NLPs was further confirmed using dynamic light scattering (DLS) and found to be  $25 \pm 3$  nm (Figure S1).

**2.4. Assembly of VAMP2 Containing Nanolipoprotein Particles (vNLP).** To generate vNLP, dried lipid film (POPC/DOPS: 85/15) was resuspended in 25 mM HEPES, pH 7.4, 140 mM KCl, 1 mM DTT, 1% OG with ApoE422K and His<sup>6</sup>-SUMO-VAMP2 at desired ratio (lipid concentration and volume same as earlier). Note: rigorous vortexing of the lipids with ApoE and VAMP2 for minimum of 3 h (can be extended up to 6 h) was found to be critical to reconstitute high copy numbers. The ApoE422K:VAMP2:lipid ratio used to get the desired copy number: 1:0.2:180 (1 copy), 1:1:180 (4 copies), 1:2:180 (8 copies), and 1:8:180 (30 copies). After the cleanup on a Superose 6 SEC column, the vNLP were concentrated (~500  $\mu$ L) and further purified from empty NLP using Ni<sup>2+</sup>-NTA beads (since only VAMP2 containing NLPs have the His<sup>6</sup> tag). The beads were washed with 20X column volume of 25 mM HEPES, pH 7.4, 140 mM KCl, 10% glycerol, 1 mM DTT with 1% OG, and the vNLP were eluted off the beads using SUMO protease (overnight at 4 °C). The vNLPs were concentrated using centrifugal filter units to ~100  $\mu$ L to a typical final concentration of 1.5 mM. The samples were analyzed by SDS-PAGE staining with Coomassie staining and the number of VAMP2 copies per NLP was determined by the VAMP2/ApoE ratio using densitometry (ImageJ) assuming six copies of ApoE422K per 1:180 NLP.<sup>33</sup> The number of copies of VAMP2 per NLP was estimated to be  $0.9 \pm 0.2$  (vNLP1),  $3.6 \pm 0.8$  (vNLP4),  $8.7 \pm 0.5$  (vNLP9), and  $30.4 \pm 2.3$  (vNLP30). SNARE-free and VAMP2 (~9 copies) containing nanodiscs (ND) were assembled and purified as previously described.<sup>26,27</sup>

**2.5. Lipid Mixing Assay.** Fusion of vNLP with small unilamellar vesicles containing t-SNARE (t-SUVs) was carried out as described previously.<sup>16,26,27</sup> vNLPs were prepared (as described above) with

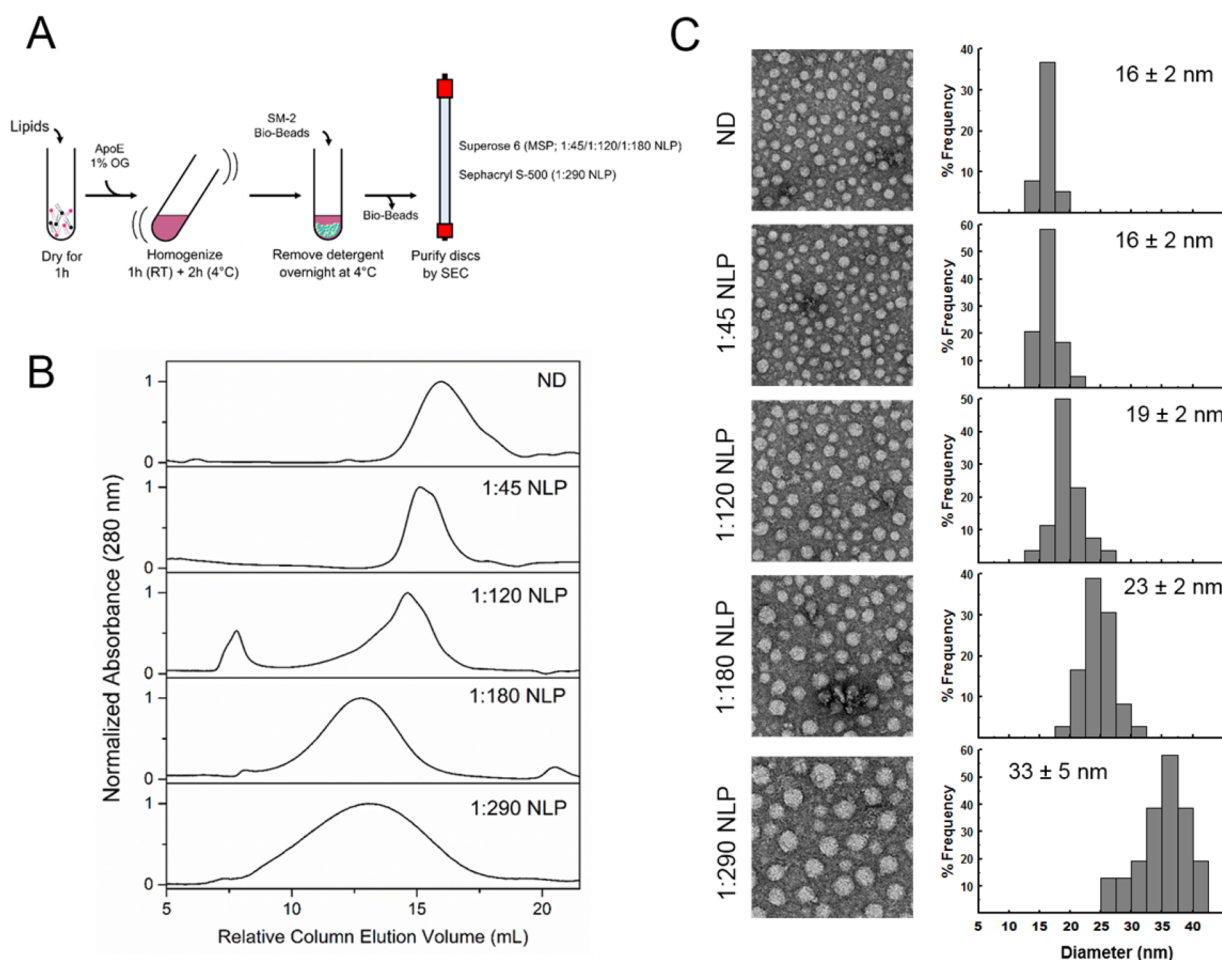


**Figure 1.** Assembly and characterization of ApoE nanolipoprotein particles. (A) Schematics of the protocol to assemble ApoE NLP complexes. (B) Elution profiles for NLPs of different ApoE/lipid ratio purified using size exclusion chromatography. The ND and 1:45, 1:120, and 1:180 NLPs were isolated on Superose 6 column and 1:290 NLPs on Sephacryl S-500 column. The relative elution volume for the two columns were calculated using the void volume of 8 and 40 mL for Superose 6 and Sephacryl S-500 columns, respectively. (C) Negative stain electron microscopy analysis of the ApoE NLPs assembled with different ApoE/lipid ratios. Representative micrographs (left) and the size distribution estimated using a minimum of 200 individual particles using ImageJ software (right) are shown.

inclusion of nitro-2,1,3-benzoxadiazol-4-yl-phosphatidylethanolamide (NBD-PE) and Rhodamine-PE (1.5 mol % each), and the fusion to t-SUV was monitored using the dequenching of NBD fluorescence (Ex 460/Em 538). Typically, 10  $\mu$ L of vNLP was mixed with 40  $\mu$ L of t-SUVs and fluorescence measured for 90 min. Thus, a typical fusion assay contains 2.5  $\mu$ M of VAMP2/0.3 mM lipids (1:125 VAMP2/lipid ratio) mixed with 7.5  $\mu$ M of t-SNARE/3 mM lipids (1:400 t-SNARE/lipid ratio). As a control, SNARE-free NLP (sf-NLP) and 10  $\mu$ M of the cytoplasmic domain of VAMP2 (CDV) were included. All fusion assays were carried out using a SpectraMax microplate reader (Molecular Devices, Sunnyvale, CA).

**2.6. Calcium Release Assay.** To measure the efflux of calcium ions ( $\text{Ca}^{2+}$ ) through the fusion pore, calcium (50 mM) encapsulated liposomes containing t-SNAREs were prepared as previously described.<sup>26,27</sup> vNLPs (10  $\mu$ L) were fused with  $\text{Ca}^{2+}$ -loaded t-SUV (40  $\mu$ L), and the release of  $\text{Ca}^{2+}$  ions through the fusion pore was tracked using 2  $\mu$ M of the calcium-sensitive fluorophore, Mag-Fluo-4 included in the external medium.<sup>26,27</sup> SNARE dependence was verified using SNARE-free NLP (sf-NLP) and CDV control.

**2.7. Dithionite Assay.** To verify that vNLPs undergo full fusion with t-SUVs and the resulting fusion pore reseal, 10  $\mu$ L of vNLP containing NBD-PE (1.5%) was first allowed to fuse with 40  $\mu$ L of t-SUV for 2 h at 37 °C. After recording the baseline NBD fluorescence for 20 min, 5  $\mu$ L of 100 mM dithionite (final concentration of 10 mM) was added to the mixture, and the acquisition was continued for an additional 20 min. 10  $\mu$ L of 5% dodecylmaltoside (detergent) was then

included to allow complete quenching of the NBD signal. Dithionite quenching of SNARE-free NLP was used as a control.<sup>26,27</sup>

**2.8. Dextran Release Assay.** t-SUVs containing fluorescein-dextran were prepared as described previously<sup>37</sup> with some modifications. 1.5  $\mu$ mol of a lipid mixture of 40% DOPC, 15% DOPS, 15 mol % 1,2-(9,10)-dibromostearoyl-sn-glycero-3-phosphocholine (BrPC, Avanti Polar Lipids, Alabaster, AL), 30% cholesterol, and 0.1 mol % 1,1'-dioctadecyl-3,3,3',3'-tetramethylindodicarbocyanine Perchlorate (DiD- $\text{C}_{18}$ , Thermo Fisher Scientific, Grant Island, NY) was dried in a glass tube for 15 min under a gentle stream of nitrogen, followed by 1 h under vacuum. The lipid film was resuspended in 25 mM HEPES, pH 7.4, 140 mM KCl, 1 mM DTT buffer containing 1% OG with t-SNAREs protein (1:400 protein/lipid ratio), fluorescein-dextran: 3000 MW (10  $\mu$ M), or 10 000 MW (20  $\mu$ M), or 40 000 MW (30  $\mu$ M), to a final volume of 250  $\mu$ L by vigorous vortexing for 1 h at RT. SUVs were prepared by rapid dilution (500  $\mu$ L of 25 mM HEPES, pH 7.4, 140 mM KCl, 1 mM DTT buffer) of detergent, followed by its complete removal by overnight dialysis at 4 °C against 4 L of the same buffer. Dextran-loaded t-SUVs were separated from unincorporated dextran and free protein on a gravity packed Sepharose CL-4B column (1.5 cm  $\times$  25 cm). Typically, the dextran loaded SUV elute at  $\sim$ 8 mL, and the final lipid concentration was 1–2 mM as determined by DiD- $\text{C}_{18}$  (622 nm) fluorescence. DLS measurements showed that average size of t-SNARE liposomes were  $\sim$ 140  $\pm$  5 nm, with or without encapsulated dextran (Figure S1), confirming the dextran does not affect the size of



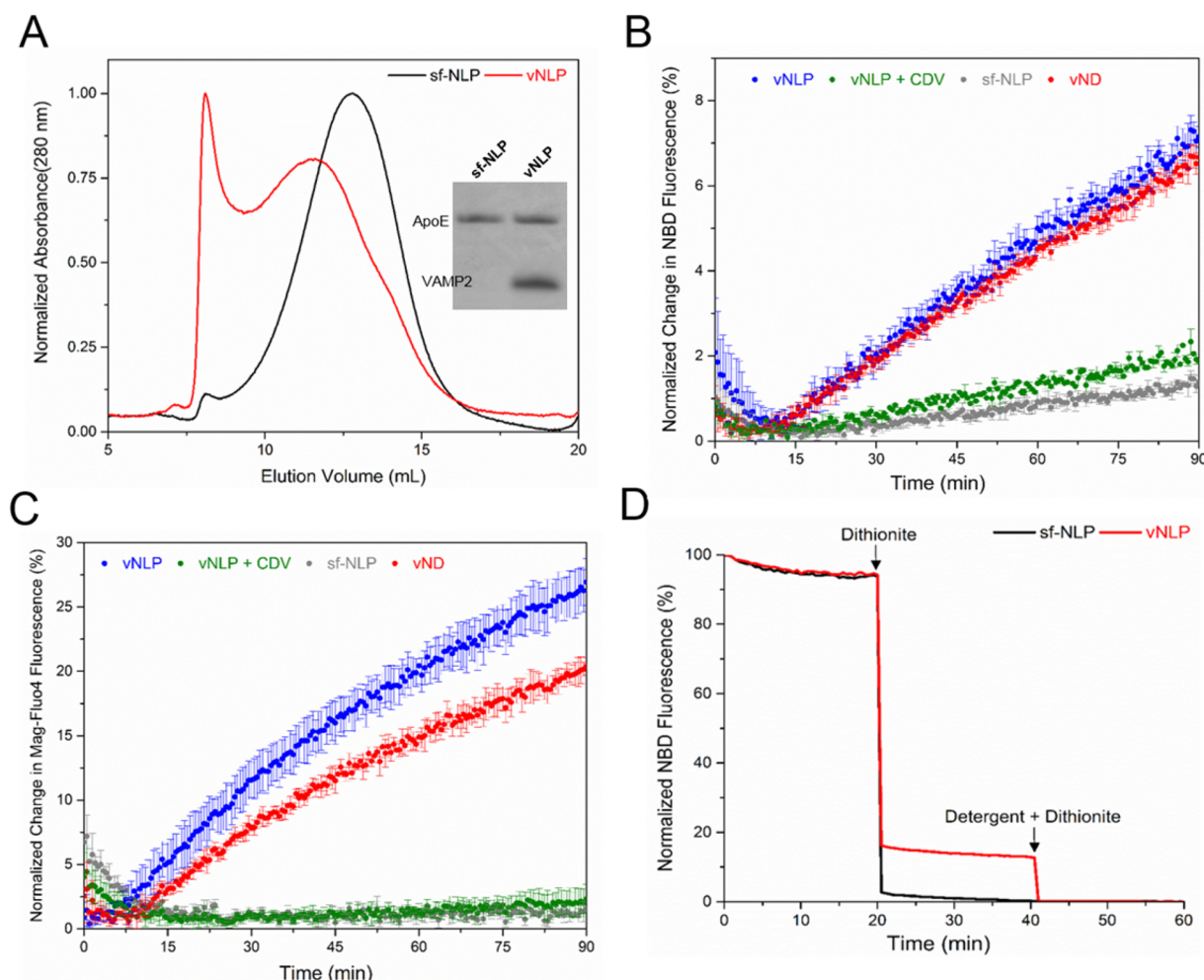


**Figure 2.** VAMP2 containing NLPs (vNLPs) as fusion partners. (A) Elution profiles of empty and VAMP2 containing NLPs on Superose 6 SEC column. Inset: Coomassie stain SDS-PAGE analysis of the elution peaks. (B) Lipid mixing monitored by dequenching of NBD fluorescence following the fusion of vNLP containing NBD and Rhodamine to acceptor t-SUVs.<sup>16</sup> (C) Formation of the fusion pore monitored by the efflux of calcium entrapped in the t-SUVs by inclusion of calcium-sensitive fluorophore, Mag-Fluo-4 in the external medium.<sup>27</sup> In both cases, Nanodiscs containing same number (~9 copies) of VAMP2 (red curve) is shown for comparison and control experiments with SNARE-free NLPs (gray) or addition of cytoplasmic domain of VAMP2 (CDV, green) are also included (D) Some NBD fluorescence included in the NLPs was protected from dithionite added externally after fusion for vNLPs (red), confirming that they undergo full fusion and that the fusion pore reseal effectively. In contrast, it is completely quenched with SNARE-free NLP (black).

the t-SNARE liposomes. Fluorescence analysis of fluorescein–dextran showed similar amounts of dextrans of all sizes were encapsulated (Figure S2). To measure the release of dextran, 80  $\mu$ L of t-SUVs loaded with 3000 MW, 10 000 MW, and 40 000 MW dextran was mixed with 20  $\mu$ L of vNLP or vND or SNARE-free NLP (as control) for 2 h at 37  $^{\circ}$ C. Samples were then diluted to 500  $\mu$ L with 25 mM HEPES, pH 7.4, 140 mM KCl, 1 mM DTT buffer and centrifuged at 85 000  $g$  for 40 min. After careful removal of the supernatant, the pellet was resuspended to 500  $\mu$ L with 25 mM HEPES, pH 7.4, 140 mM KCl, 1 mM DTT buffer. The lipids in both supernatant and the pellet fractions were completely solubilized by addition of detergent (1% OG) with vortexing for 1 h at RT. Subsequently, fluorescein (490 nm) and DiD (622 nm) fluorescence in the supernatant and pellet fractions were used to estimate the amount of dextran and lipid in each fraction. The efficiency of vesicle pelleting was generally about 90–95%. The percent dextran released was corrected for the incomplete pelleting and was calculated using the formula

$$\text{dextran released (\%)} = \left[ \frac{F_{dx-sup}}{F_{dx-sup} + F_{dx-pel}} - \frac{F_{lip-sup}}{F_{lip-sup} + F_{lip-pel}} \right] \times 100$$

where  $F_{dx-sup}$  and  $F_{lip-sup}$  are the dextran (fluorescein) and lipid (DiD) fluorescence in the supernatant and  $F_{dx-pel}$  and  $F_{lip-pel}$  are the dextran (fluorescein) and lipid (DiD) fluorescence in the pellet fraction. The dextran release (%) were also corrected for nonspecific release due to leakiness/or lysis using the SNARE-free NLP (control) sample.

### 3. RESULTS

**3.1. Assembly and Characterization of ApoE Nanolipoprotein Particles.** To assemble soluble nanometer-sized lipid discs, large enough to allow the expansion of a fusion pore, we used apolipoprotein E (ApoE) as it has been shown to self-assemble with lipids to form a mixture of different sized nanolipoprotein complexes.<sup>32–34</sup> We reasoned that by controlling the ApoE/lipid ratio, we could template the size of the NLPs. So, we assembled the NLPs from apoE422K (the N-terminal 22 kDa fragment of apolipoprotein E4) and a lipid mixture of POPC/DOPS at 85:15 in the presence of detergent (1% octylglucoside) for varying ApoE/lipid ratios to identify the ideal condition (Figure 1A). Following removal of detergent, the assembled NLPs were purified from free proteins

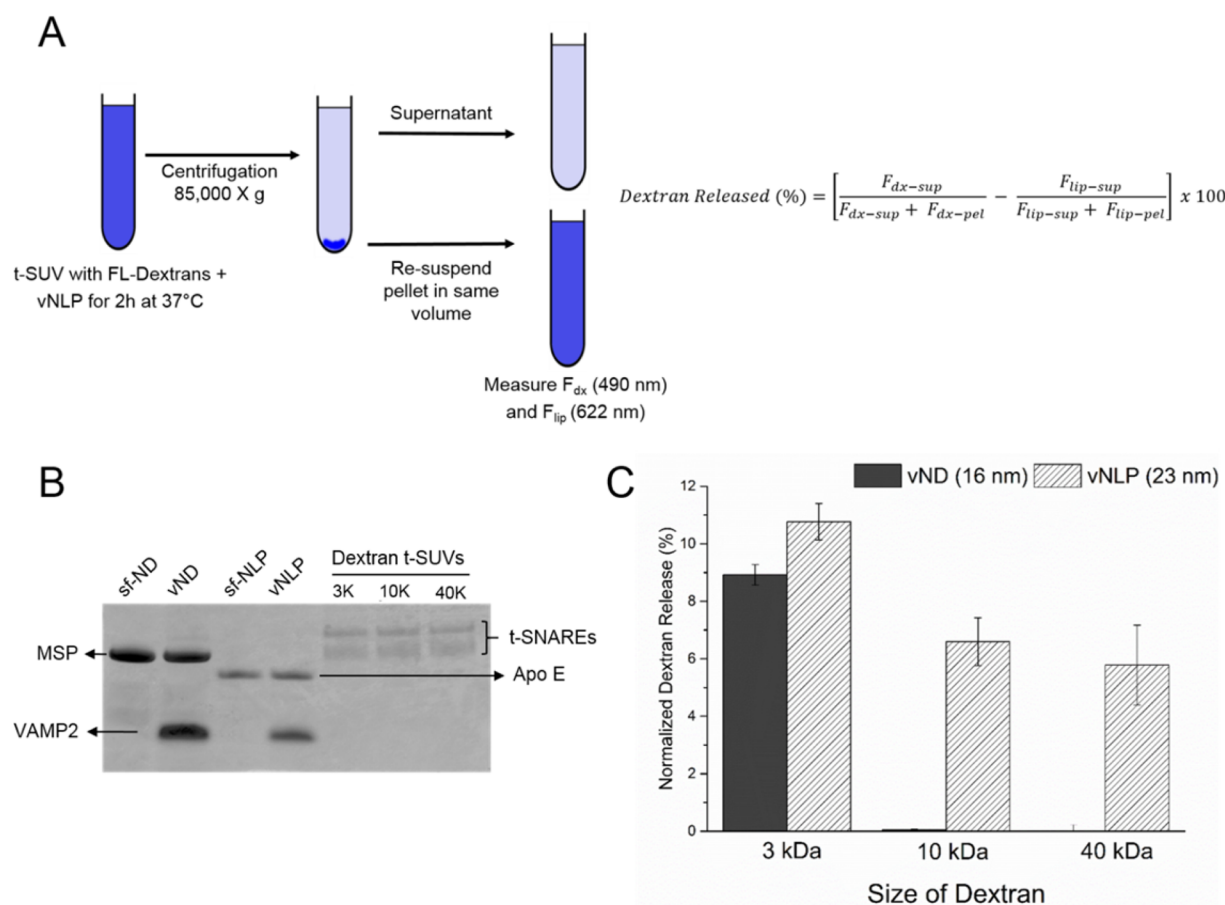


**Figure 3.** NLPs accommodate the dilation of the fusion pore. (A) Schematics of the dextran release assay. Amount of encapsulated dextrans 3000 MW (Stokes radius  $\sim 1$  nm), 10 000 MW ( $\sim 2.3$  nm), and 40 000 MW ( $\sim 4.4$  nm) released in to the supernatant after fusion with vNLPs was estimated following pelleting of the vesicles. The dextran released (%) was corrected for inefficient pelleting and for nonspecific leakiness/lysis. (B) SDS-PAGE analysis confirms that equal amounts of t-SNAREs have been incorporated in each dextran containing t-SUVs. The SNARE-free and VAMP2 (nine copies) containing ND and NLP used in this analysis are also shown (C) Normalized dextran released in the medium shows that dextrans of all sizes are efficiently released with NLPs as compared to the NDs, confirming that NLPs accommodate expansion of the nucleated fusion pore up to at least  $\sim 9$  nm.

and lipids by size-exclusion chromatography, and the size distribution was analyzed using negative stain EM (Figure 1A).

We systematically varied the ApoE/lipid ratio from 1:40 to 1:300 while maintaining the lipid concentration constant, but homogeneous NLP particles of discrete sizes were observed only for certain ratios (Figure 1B). This is consistent with the earlier observation that only certain sizes of NLPs are stable and is determined by the available folding conformers of the ApoE protein.<sup>33</sup> NLPs assembled with a high ApoE/lipid ratio (1:45) were smaller in size, with elution profile comparable to that of ApoA1 derived nanodiscs (Figure 1B). With decreasing ApoE/lipid ratio, the NLPs eluted progressively earlier on the SEC columns (Figure 1B), consistent with increasing size. This was confirmed by negative stain EM analysis, with an estimated diameters centered at  $\sim 16$ , 19, 23, and 33 nm for ApoE/lipid ratios of 1:45, 1:120, 1:180, and 1:290, respectively (Figure 1C). Additionally, the EM analysis showed that the particle size distribution for NLPs up to ApoE:lipid ratio of 1:180 were monodisperse ( $\pm 2$  nm), but 1:290 NLPs had a broader size ( $\pm 5$  nm) distribution (Figure 1C). Although the 1:290 NLPs were polydisperse, it eluted as a single peak in the Sephacryl-S500 column used (Figure 1B). We were unable to resolve the different sized particles within the elution peak since the large size of the NLPs precludes it from being purified on high

resolution SEC columns like Superose 6 used for the other NLPs. Therefore, the ApoE/lipid ratio of 1:180 was found to be the best condition to generate large ( $\sim 23$  nm) and monodisperse NLPs. Larger NLPs can be produced if heterogeneity is a not an issue for the intended use.

On the basis of previous modeling and molecular dynamics simulation studies,<sup>33</sup> we estimate that the 1:180 NLPs are made up of 6 ApoE protein and  $\sim 1250$  lipid molecules. From negative stain EM images (Figure S3), it is quite apparent that the 1:180 NLPs are pure lipid discs, free of contamination with liposomes and other lipid particles, and this was confirmed by the dithionite quenching assay (Figure 2C, see below). Further, we found that the composition of the lipid has only a minor effect on the size of the NLPs, as 1:180 NLPs assembled with POPC alone or DMPC alone or a physiologically relevant lipid mixture (32% POPC, 15% DOPS, 23% POPE, 25% cholesterol, 3% PI, and 2% PIP2) yielded NLPs of comparable size and homogeneity (Figure S4).

**3.2. ApoE Nanolipoprotein Particles as Fusion Partners.** To assess if 1:180 NLPs (henceforth referred simply as “NLPs”) are suitable as fusion partners, synaptic v-SNARE (VAMP2) was incorporated into them. VAMP2-containing NLP (vNLP) were prepared by including the VAMP2 protein during NLP reconstitution and purified from empty NLPs and



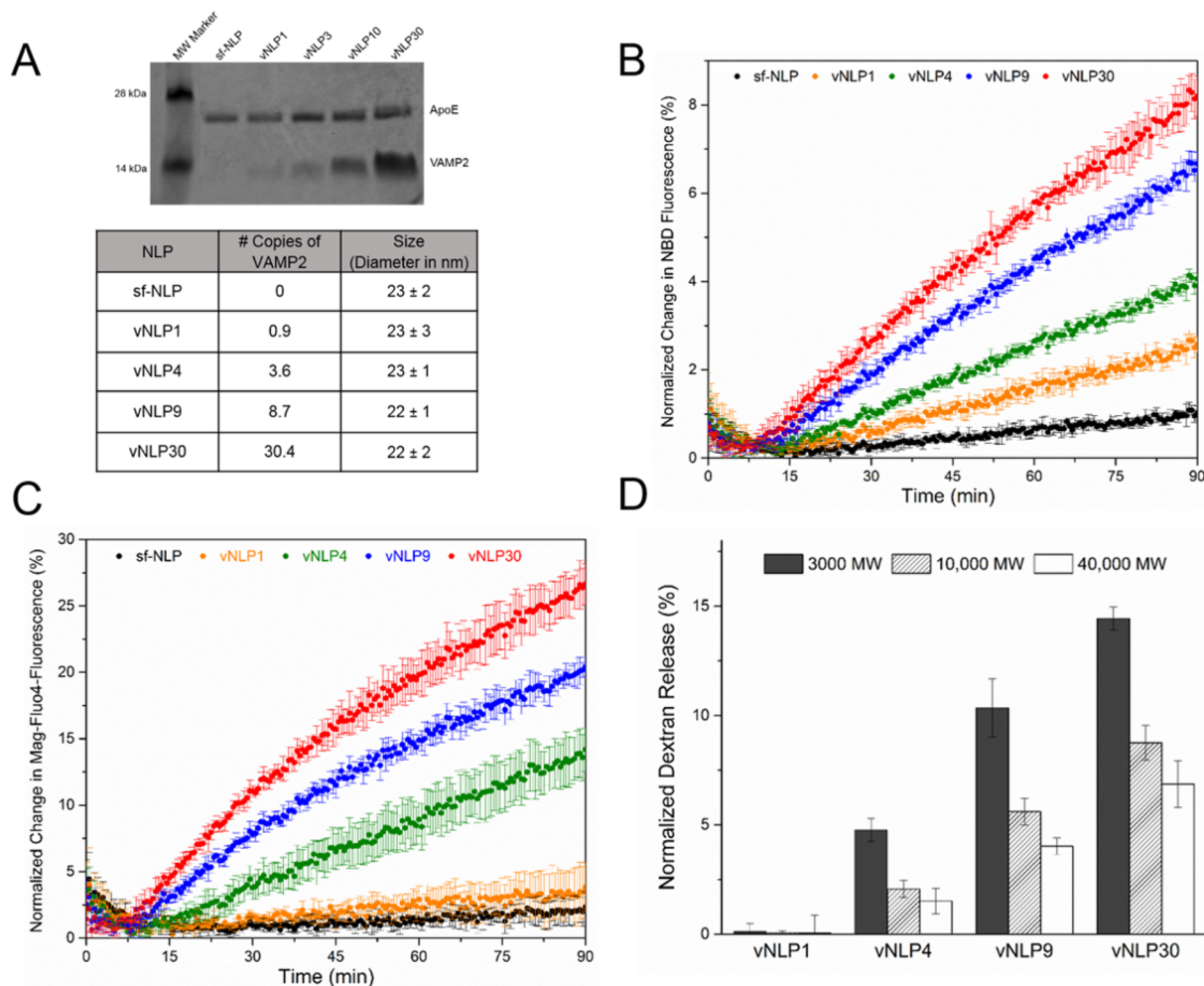


**Figure 4.** Effect of VAMP2 copy number on fusion pore dynamics. (A) NLPs with desired number of VAMP2 copy was generated by adjusting the ApoE/VAMP2 input ratio. Based on the coomassie stained SDS-PAGE analysis, the number of copies of VAMP2 per NLP was estimated by densitometry assuming each NLP is formed by 6 copies of ApoE protein. The size and particle distribution of vNLPs were determined by negative stain EM analysis. (B) All vNLPs tested drove lipid mixing as monitored by NBD dequenching assay, with rate and extent of fusion correlated to the copy number. (C) Calcium release assays of vNLP with different VAMP2 copies shows efficient efflux starting with NLP containing at least 3–4 copies of VAMP2 (vNLP4), with little or no calcium efflux was detectable with lower copy number (vNLP1, orange curve). (D) Dextran release assay shows that increasing the number of copies of VAMP2 per NLP enhances the efflux of dextran, including the larger (10 000 MW and 40 000 MW) dextrans indicating a cooperative role for SNAREs in dilating the fusion pore.

free proteins/lipids by SEC, followed by Ni-NTA affinity purification (Figure 2A). We used a well-established lipid mixing assay<sup>16,26,27</sup> to test whether the vNLP can fuse with small unilamellar vesicles containing the cognate t-SNARE complex of Syntaxin1 and SNAP25 (t-SUV). Fusion of the vNLP with the t-SUV can be monitored by dequenching of NBD fluorescence due to substantial dilution of vNLP lipids.<sup>16,26,27</sup> As shown in Figure 2B, we observed robust fusion of the 23 nm vNLP with ~9 copies of VAMP2 to the t-SUV, with fusion levels comparable to the 16 nm vNDs loaded to its maximal capacity of VAMP2 (~9 copies, vND<sup>27</sup>). In contrast, there was little or no increase in NBD fluorescence in control experiments with either SNARE-free NLP (sf-NLP) or when the cytoplasmic domain of VAMP (CDV) was included to titrate out the t-SNAREs. This shows that the NLPs are not inherently fusogenic and the cognate SNAREs are required to catalyze fusion. A similar fusion process was observed when the SNARE topology was reversed, with t-SNAREs in NLP and VAMP2 in the vesicles (Figure S5).

Next, we adapted a previously described experimental setup using calcium-loaded vesicles and a calcium-sensitive fluorophore, Mag-Fluo-4 included in the external medium to monitor the release of cargo through a SNARE-induced fusion pore.<sup>26,27</sup> When vNLP fuses with the calcium-loaded t-SUVs, the calcium diffuses through the resulting fusion pore into the exterior buffer, with a consequent increase in Mag-Fluo-4 fluorescence, as we observed in Figure 2C. This data also highlights the stability of the NLPs as calcium efflux was found to be strictly dependent on the cognate SNAREs. To verify that the SNARE induced fusion pores on vNLP can reseal, we used the dithionite protection assay.<sup>26,27</sup> Dithionite added externally (at the end of the fusion assay) will fully quench all NBD on unreacted NLPs (as both leaflets are accessible to the exterior medium) and any NBD-PE that the diffused on to the outer leaflet of the liposome via membrane fusion. If the fusion pore remains open for extended periods of time, then dithionite can also diffuse through and quench the NBD on the inner leaflet also. However, we observed that some of the NBD dye remained protected against dithionite (Figure 2D), confirming

that vNLP can undergo full fusion, with a fusion pore that can reseal. Further, this data indicated that ~40% of all fusion events result in full fusion with subsequent resealing of the pore, while the balance maybe be events resembling hemifusion, in which only the outer leaflets are merged. This is consistent with that observed in the ND-liposome fusion assays.<sup>27</sup>

**3.3. ApoE Nanolipoprotein Particles Accommodate Expansion of the Fusion Pore.**  $\text{Ca}^{2+}$  ions are small enough that they can readily diffuse through the nascent fusion pore (~2 nm); so to ascertain that NLPs can indeed accommodate the expansion of the fusion pore, we tested the release of encapsulated dextran of different sizes.<sup>37</sup> We encapsulated fluorescein-labeled dextran of 3000 MW (Stokes radius ~1 nm), 10 000 MW (Stokes radius ~2.3 nm), and 40 000 MW (Stokes radius ~4.4 nm) in the t-SNARE liposomes, which was then incubated with vNLP (or vND as control) for 2 h at 37 °C. The amount of fluorescein–dextran released into the medium was quantitated after pelleting the vesicles by centrifugation (Figure 3A). We examined the pore size in t-SUVs composed of DOPC/BrPC/cholesterol. BrPC (15%), a high density lipid, was included to assist in efficient pelleting of the t-SUVs, and cholesterol (30%) was required for efficient trapping of the dextran and also made the t-SUVs less leaky. In control experiments with 16 nm vND, we detected an efficient release of the 3000 MW dextran into the external medium (~10% after corrected for nonspecific release due to leakiness/limited lysis), but little or no efflux of the larger 10 000 MW and 40 000 MW dextrans (Figure 3C) even though all vesicles had the same amount of t-SNAREs (Figure 3B). This is consistent with the properties of the NDs which allow for the nucleation of the fusion pore (~2 nm diameter), but the nascent pore cannot expand appreciably.<sup>27</sup> In contrast, we observed efflux of dextran of all three sizes into the external medium (Figure 3C) for the 23 nm vNLP loaded with same number of VAMP2 (~9 copies), and the percent of dextran released was correlated to the size of the encapsulated dextran (~11%, 7%, and 5% for 3000 MW, 10 000 MW, and 40 000 MW respectively). These data clearly show that vNLP allow the expansion of fusion pore up to at least ~9 nm.

**3.4. Effect of Number of Copies of VAMP2 on Fusion Pore Formation and Expansion.** A distinct advantage of the larger NLP system is that the number of copies of reconstituted protein can be tightly controlled. By adjusting the input ApoE:VAMP2 ratio, combined with the SEC and affinity purification, we could generate homogeneous vNLPs with a defined number of VAMP2. To understand the effect of SNARE copy number on the fusion pore nucleation and expansion, we produced vNLPs containing at average 0.9 (vNLP1), 3.6 (vNLP4), 8.7 (vNLP9), and 30.4 (vNLP30) copies of VAMP2 (Figure 4A). As expected, the capacity of the larger NLPs vastly exceeds that of the smaller NDs as the maximal copies of VAMP2 incorporated in the NLPs was ~30 compared to ~9 for the NDs. EM analysis confirmed that the VAMP2 reconstitution does not affect the size or the homogeneity of the vNLPs (Figure 4A) as all vNLP samples were monodisperse and similarly sized (~23 ± 2 nm).

All vNLPs tested drove lipid mixing (as measured by NBD dequenching) and the rate and extent of lipid mixing corresponding to the number of copies of VAMP2 in the NLP (Figure 4B). In contrast, efficient efflux of  $\text{Ca}^{2+}$  was observed only with 3–4 copies of VAMP2 per NLP (vNLP4), and the amount of release increased with the VAMP2 copy

number. There was very little or no content released for vNLPs containing ~1 copy of VAMP2 (Figure 4B, orange curve). To rule out that this is due to deficient docking of vNLP1, we tested and confirmed that vNLP1, even following overnight preincubation with t-SUVs on ice, does not support efflux of cargo (Figure S6). The lipid mixing and  $\text{Ca}^{2+}$ -release results are consistent with earlier *in vitro* and *in vivo* observations that 1 copy of SNARE protein is sufficient to drive lipid mixing, but ~3–4 SNAREs are needed for efficient content release.<sup>38–40</sup> Interestingly, with the vNLPs, the  $\text{Ca}^{2+}$  release did not saturate at ~7 copies of VAMP2 as previously observed with nanodiscs.<sup>27</sup> This may be the consequence of the expansion of the initial fusion pore accommodated in the 23 nm NLPs, but not in the 16 nm NDs. If so, then it hints at a direct role for SNAREs density in driving the expansion of the nascent fusion pore. To verify this, we compared the efflux of encapsulated dextrans (3000 MW, 10 000 MW, and 40 000 MW) for all vNLPs. Of particular interest was the efflux of larger 10 000 MW and 40 000 MW dextrans as they are released only following the expansion of the fusion pore. As shown in Figure 4D, we detected a higher percent of dextrans of all sizes released into the external medium with increasing number of VAMP2 per NLP, starting with vNLP4. Taken together, the data confirm that ~3–4 copies of VAMP2 are needed to open a fusion pore, and the SNARE proteins also act cooperatively to dilate this nascent fusion pore.

## 4. DISCUSSION

The NLP–liposome system demonstrated here shares many key characteristics with the previously described nanodisc–liposome setup to study fusion pores.<sup>26,27</sup> Like the NDs, the fusion pores in the NLPs are externally accessible, which allows for direct and reliable characterization of the pore properties. Similarly, in this biochemically defined system, the size of the NLPs, the lipid composition, the identity, and number of copies of the protein to be incorporated can all be rigorously controlled, making it very versatile yet reliable setup.

The NLPs goes further in addressing some of the limitation of the NDs. Unlike the NDs, the large larger size of the NLPs allow the expansion of the nucleated fusion pore with efficient efflux of large cargoes, as we observed release of dextrans up to ~9 nm in diameter (Figure 3C). Nevertheless, these larger pores are dynamic and ultimately reseal as evidenced by a dithionite protection assay (Figure 2D). Thus, NLPs expand the applicability of this *in vitro* system to study efflux of larger cargo molecules like hormones, peptides, and viral genomes. In addition, the NLPs have the capacity to accommodate a larger number of proteins as compared to the NDs, while maintaining a tight control on the number of the proteins incorporated. In fact, we were able to successfully isolate monodisperse NLPs with ~30 copies of the VAMP2 protein without affecting the size of the NLPs (Figure 4A). These characteristics make the NLPs perfectly suited to investigate both nucleation and the fate of the nucleated pore, in particular to delineate the key elements that influence the dynamics of the fusion pore, like the nature and number of the fusogens, the effect of regulatory protein(s), and the lipid composition.

Using this system, we examined the role of SNARE density on fusion pore nucleation and its dilation and find that ~3–4 copies of SNARE proteins (2 SNARE per face of the NLP) are needed to keep the fusion pore open, and the SNAREs act cooperatively to expand the fusion pore, as increasing the number of SNAREs per NLP resulted in enhanced efflux of



10 000 MW and 40 000 MW dextrans (Figure 4). Direct measurements of vNLP fusion pores using electrophysiological assay, which is focus of a collaborative manuscript under review,<sup>41</sup> corroborate our findings that only a few SNARE complexes are required to nucleate a fusion pore and the probability of pore dilation increases with SNARE density, with well above a dozen SNAREs required to reliably dilate the nascent pore.<sup>41</sup> This article also explores the properties of the single fusion pores on vNLP and presents detailed analysis of single-pore statistics.<sup>41</sup>

Besides the fusion pore analysis, we envision additional applications for the ApoE NLPs. Of particular interest is NLPs as scaffolds to solubilize large membrane proteins and membrane protein complexes. The high capacity of the NLPs due to inherent conformational flexibility of ApoE molecule<sup>33</sup> allows for large molecular complexes, with multiple membrane spanning segments to be reconstituted. In our attempts, we have been able to generate NLP as large as 40 nm with up to ~75 copies of VAMP2 reconstituted (data not shown). These complexes are typically more polydisperse, so we did not pursue them further in this study. The ability for NLPs to accommodate a large protein complexes with a deformable membrane pore readily lends itself for structural and functional studies in variety of disciplines including, membrane channels, pore-forming toxins, antimicrobial peptides, and protein translocation machinery. For example, a recent study with Sec translocon showed that the high lipid environment of the NLPs (as compared to the NDs) makes SecYEG reconstituted into the NLPs highly active and support translocation at low SecA concentration [Koch, S.; Driessen, A., personal communication].

## 5. CONCLUSION

In this report, we describe new methods to template and purify monodisperse ApoE derived lipid bilayer discs of ~23 nm diameter, containing the desired numbers of reconstituted protein(s). Using *in vitro* lipid mixing and content release assays, we establish that VAMP2 containing ApoE NLPs are fusion partners to cognate t-SNARE liposomes, with the resulting fusion pore accessible to the exterior. Using this setup, we find that at least 3–4 copies (2 per face of NLP) of the v-SNARE, VAMP2 is required to open a nascent fusion pore, and the SNARE proteins act cooperatively to expand the nascent pore. In summary, the NLP–liposome setup described here represents a complete reconstituted *in vitro* system that could be employed to explicitly probe the structure and the dynamic properties of the fusion pore.

## ■ ASSOCIATED CONTENT

### Supporting Information

The Supporting Information is available free of charge on the ACS Publications website at DOI: 10.1021/acs.langmuir.6b00245.

Figures S1–S6 (PDF)

## ■ AUTHOR INFORMATION

### Corresponding Authors

\*E-mail [james.rothman@yale.edu](mailto:james.rothman@yale.edu) (J.E.R.).

\*E-mail [shyam.krishnakumar@yale.edu](mailto:shyam.krishnakumar@yale.edu) (S.S.K.).

### Notes

The authors declare no competing financial interest.

## ■ ACKNOWLEDGMENTS

We thank F. Pincet and E. Karatekin for helpful discussions and critical reading of the manuscript. This work was supported by National Institutes of Health Grant DK027044 to J.E.R.

## ■ REFERENCES

- (1) Sollner, T. H. Intracellular and viral membrane fusion: a uniting mechanism. *Curr. Opin. Cell Biol.* **2004**, *16* (4), 429–35.
- (2) Martens, S.; McMahon, H. T. Mechanisms of membrane fusion: disparate players and common principles. *Nat. Rev. Mol. Cell Biol.* **2008**, *9* (7), 543–56.
- (3) Jahn, R.; Lang, T.; Sudhof, T. C. Membrane fusion. *Cell* **2003**, *112* (4), 519–33.
- (4) Rothman, J. E. The Principle of Membrane Fusion in the Cell (Nobel Lecture). *Angew. Chem., Int. Ed.* **2014**, *53* (47), 12676–12694.
- (5) Harrison, S. C. Viral membrane fusion. *Virology* **2015**, 479–480, 498–507.
- (6) Lindau, M.; Alvarez de Toledo, G. The fusion pore. *Biochim. Biophys. Acta, Mol. Cell Res.* **2003**, *1641* (2–3), 167–73.
- (7) Jackson, M. B.; Chapman, E. R. The fusion pores of Ca<sup>2+</sup>-triggered exocytosis. *Nat. Struct. Mol. Biol.* **2008**, *15* (7), 684–9.
- (8) Kozlov, M. M.; Chernomordik, L. V. Membrane tension and membrane fusion. *Curr. Opin. Struct. Biol.* **2015**, *33*, 61–67.
- (9) He, L.; Wu, X. S.; Mohan, R.; Wu, L. G. Two modes of fusion pore opening revealed by cell-attached recordings at a synapse. *Nature* **2006**, *444* (7115), 102–5.
- (10) Staal, R. G.; Mosharov, E. V.; Sulzer, D. Dopamine neurons release transmitter via a flickering fusion pore. *Nat. Neurosci.* **2004**, *7* (4), 341–6.
- (11) Vardjan, N.; Jorgacevski, J.; Stenovec, M.; Kreft, M.; Zorec, R. Compound exocytosis in pituitary cells. *Ann. N. Y. Acad. Sci.* **2009**, *1152*, 63–75.
- (12) Spruce, A. E.; Iwata, A.; White, J. M.; Almers, W. Patch clamp studies of single cell-fusion events mediated by a viral fusion protein. *Nature* **1989**, *342* (6249), 555–8.
- (13) Vardjan, N.; Jorgacevski, J.; Zorec, R. Fusion pores, SNAREs, and exocytosis. *Neuroscientist* **2013**, *19* (2), 160–74.
- (14) Michael, D. J.; Cai, H.; Xiong, W.; Ouyang, J.; Chow, R. H. Mechanisms of peptide hormone secretion. *Trends Endocrinol. Metab.* **2006**, *17* (10), 408–15.
- (15) Sollner, T.; Whiteheart, S. W.; Brunner, M.; Erdjument-Bromage, H.; Geromanos, S.; Tempst, P.; Rothman, J. E. SNAP receptors implicated in vesicle targeting and fusion. *Nature* **1993**, *362* (6418), 318–24.
- (16) Weber, T.; Zemelman, B. V.; McNew, J. A.; Westermann, B.; Gmachl, M.; Parlati, F.; Sollner, T. H.; Rothman, J. E. SNAREpins: minimal machinery for membrane fusion. *Cell* **1998**, *92* (6), 759–72.
- (17) Melia, T. J.; Weber, T.; McNew, J. A.; Fisher, L. E.; Johnston, R. J.; Parlati, F.; Mahal, L. K.; Sollner, T. H.; Rothman, J. E. Regulation of membrane fusion by the membrane-proximal coil of the t-SNARE during zippering of SNAREpins. *J. Cell Biol.* **2002**, *158* (5), 929–40.
- (18) Li, F.; Pincet, F.; Perez, E.; Eng, W. S.; Melia, T. J.; Rothman, J. E.; Tareste, D. Energetics and dynamics of SNAREpin folding across lipid bilayers. *Nat. Struct. Mol. Biol.* **2007**, *14* (10), 890–6.
- (19) Ji, H.; Coleman, J.; Yang, R.; Melia, T. J.; Rothman, J. E.; Tareste, D. Protein determinants of SNARE-mediated lipid mixing. *Biophys. J.* **2010**, *99* (2), 553–60.
- (20) Ma, C.; Su, L.; Seven, A. B.; Xu, Y.; Rizo, J. Reconstitution of the vital functions of Munc18 and Munc13 in neurotransmitter release. *Science* **2013**, *339* (6118), 421–5.
- (21) Bowen, M. E.; Weninger, K.; Brunger, A. T.; Chu, S. Single molecule observation of liposome-bilayer fusion thermally induced by soluble N-ethyl maleimide sensitive-factor attachment protein receptors (SNAREs). *Biophys. J.* **2004**, *87* (5), 3569–84.
- (22) Kyoung, M.; Srivastava, A.; Zhang, Y.; Diao, J.; Vrljic, M.; Grob, P.; Nogales, E.; Chu, S.; Brunger, A. T. In vitro system capable of differentiating fast Ca<sup>2+</sup>-triggered content mixing from lipid exchange



for mechanistic studies of neurotransmitter release. *Proc. Natl. Acad. Sci. U. S. A.* **2011**, *108* (29), E304–13.

(23) Alabi, A. A.; Tsien, R. W. Perspectives on kiss-and-run: role in exocytosis, endocytosis, and neurotransmission. *Annu. Rev. Physiol.* **2013**, *75*, 393–422.

(24) Lindau, M. High resolution electrophysiological techniques for the study of calcium-activated exocytosis. *Biochim. Biophys. Acta, Gen. Subj.* **2012**, *1820* (8), 1234–42.

(25) Xu, Y.; Rubin, B. R.; Orme, C. M.; Karpikov, A.; Yu, C.; Bogan, J. S.; Toomre, D. K. Dual-mode of insulin action controls GLUT4 vesicle exocytosis. *J. Cell Biol.* **2011**, *193* (4), 643–53.

(26) Shi, L.; Howan, K.; Shen, Q. T.; Wang, Y. J.; Rothman, J. E.; Pincet, F. Preparation and characterization of SNARE-containing nanodiscs and direct study of cargo release through fusion pores. *Nat. Protoc.* **2013**, *8* (5), 935–48.

(27) Shi, L.; Shen, Q. T.; Kiel, A.; Wang, J.; Wang, H. W.; Melia, T. J.; Rothman, J. E.; Pincet, F. SNARE proteins: one to fuse and three to keep the nascent fusion pore open. *Science* **2012**, *335* (6074), 1355–9.

(28) Bayburt, T. H.; Sligar, S. G. Self-assembly of single integral membrane proteins into soluble nanoscale phospholipid bilayers. *Protein science: a publication of the Protein Society* **2003**, *12* (11), 2476–81.

(29) Jonas, A. Reconstitution of high-density lipoproteins. *Methods Enzymol.* **1986**, *128*, 553–82.

(30) Jonas, A.; Sweeny, S. A.; Herbert, P. N. Discoidal complexes of A and C apolipoproteins with lipids and their reactions with lecithin: cholesterol acyltransferase. *J. Biol. Chem.* **1984**, *259* (10), 6369–75.

(31) Chromy, B. A.; Arroyo, E.; Blanchette, C. D.; Bench, G.; Benner, H.; Cappuccio, J. A.; Coleman, M. A.; Henderson, P. T.; Hinz, A. K.; Kuhn, E. A.; Pesavento, J. B.; Segelke, B. W.; Sulchek, T. A.; Tarasow, T.; Walsworth, V. L.; Hoeprich, P. D. Different apolipoproteins impact nanolipoprotein particle formation. *J. Am. Chem. Soc.* **2007**, *129* (46), 14348–54.

(32) Blanchette, C. D.; Cappuccio, J. A.; Kuhn, E. A.; Segelke, B. W.; Benner, W. H.; Chromy, B. A.; Coleman, M. A.; Bench, G.; Hoeprich, P. D.; Sulchek, T. A. Atomic force microscopy differentiates discrete size distributions between membrane protein containing and empty nanolipoprotein particles. *Biochim. Biophys. Acta, Biomembr.* **2009**, *1788* (3), 724–31.

(33) Blanchette, C. D.; Law, R.; Benner, W. H.; Pesavento, J. B.; Cappuccio, J. A.; Walsworth, V.; Kuhn, E. A.; Corzett, M.; Chromy, B. A.; Segelke, B. W.; Coleman, M. A.; Bench, G.; Hoeprich, P. D.; Sulchek, T. A. Quantifying size distributions of nanolipoprotein particles with single-particle analysis and molecular dynamic simulations. *J. Lipid Res.* **2008**, *49* (7), 1420–30.

(34) Blanchette, C. D.; Segelke, B. W.; Fischer, N.; Corzett, M. H.; Kuhn, E. A.; Cappuccio, J. A.; Benner, W. H.; Coleman, M. A.; Chromy, B. A.; Bench, G.; Hoeprich, P. D.; Sulchek, T. A. Characterization and purification of polydisperse reconstituted lipoproteins and nanolipoprotein particles. *Int. J. Mol. Sci.* **2009**, *10* (7), 2958–71.

(35) Krishnakumar, S. S.; Kummel, D.; Jones, S. J.; Radoff, D. T.; Reinisch, K. M.; Rothman, J. E. Conformational dynamics of calcium-triggered activation of fusion by synaptotagmin. *Biophys. J.* **2013**, *105* (11), 2507–16.

(36) Morrow, J. A.; Arnold, K. S.; Weisgraber, K. H. Functional characterization of apolipoprotein E isoforms overexpressed in *Escherichia coli*. *Protein Expression Purif.* **1999**, *16* (2), 224–30.

(37) Lin, Q.; Wang, T.; Li, H.; London, E. Decreasing Transmembrane Segment Length Greatly Decreases Perfringolysin O Pore Size. *J. Membr. Biol.* **2015**, *248* (3), 517–27.

(38) van den Bogaart, G.; Holt, M. G.; Bunt, G.; Riedel, D.; Wouters, F. S.; Jahn, R. One SNARE complex is sufficient for membrane fusion. *Nat. Struct. Mol. Biol.* **2010**, *17* (3), 358–64.

(39) Hua, Y.; Scheller, R. H. Three SNARE complexes cooperate to mediate membrane fusion. *Proc. Natl. Acad. Sci. U. S. A.* **2001**, *98* (14), 8065–70.

(40) Mohrmann, R.; de Wit, H.; Verhage, M.; Neher, E.; Sorensen, J. B. Fast vesicle fusion in living cells requires at least three SNARE complexes. *Science* **2010**, *330* (6003), 502–5.

(41) Wu, Z.; Bello, O.; Auclair, S. M.; Vennekate, W.; Krishnakumar, S. S.; Karatekin, E. Dilation of fusion pores by soluble N-ethylmaleimide-sensitive factor attachment protein receptor (SNARE) proteins. Manuscript submitted.